Translational Oncology
www.transonc.com

Volume 13 Number 2 February 2020 pp. 254–261 254

Ultrasound Guided Optoacoustic Tomography in Assessment of Tumor Margins for Lumpectomies

Yonggeng Goh[*,1], Ghayathri Balasundaram[†,1], Mohesh Moothanchery[†], Amalina Attia[†], Xiuting Li[†], Hann Qian Lim[†], Neal C. Burton[‡], Yi Qiu[‡], Thomas Choudary Putti[§], Ching Wan Chan[¶], Philip Iau[¶], Shaik Ahmad Buhari[¶], Mikael Hartman[¶], Siau Wei Tang[¶], Celene Wei Qi Ng[¶], Yiong Huak Chan[#], Felicity Jane Pool[*], Premilla Pillay[*], Wynne Chua[*], Jeevesh Kapur[*], Pooja Jagmohan[*], Eide Sterling[*], Swee Tian Quek[*] and Malini Olivo[†]

[*]Department of Diagnostic Imaging, National University Hospital, Singapore; [†]Laboratory of Bio-Optical Imaging, Singapore Bioimaging Consortium, Singapore; [‡]IThera Medical GmbH, Germany; [§]Department of Pathology, National University Hospital, Singapore; [¶]Department of Breast Surgery, National University Hospital, Singapore; [#]Department of Biostatistics, Yong Loo Lin School of Medicine, National University of Singapore, Singapore

Abstract

PURPOSE: To determine the accuracy of a handheld ultrasound-guided optoacoustic tomography (US-OT) probe developed for human deep-tissue imaging in ex vivo assessment of tumor margins postlumpectomy. **METHODS**: A custom-built two-dimensional (2D) US-OT—handheld probe was used to scan 15 lumpectomy breast specimens. Optoacoustic signals acquired at multiple wavelengths between 700 and 1100 nm were reconstructed using model linear algorithm, followed by spectral unmixing for lipid and deoxyhemoglobin (Hb). Distribution maps of lipid and Hb on the anterior, posterior, superior, inferior, medial, and lateral margins of the specimens were inspected for margin involvement, and results were correlated with histopathologic findings. The agreement in tumor margin assessment between US-OT and histopathology was determined using the Bland—Altman plot. Accuracy, sensitivity, specificity, positive predictive value (PPV), and negative predictive value (NPV) of margin assessment using US-OT were calculated. **RESULTS**: Ninety margins (6 × 15 specimens) were assessed. The US-OT probe resolved blood vessels and lipid up to a depth of 6 mm. Negative and positive margins were discriminated by marked differences in the distribution patterns of lipid and Hb. US-OT assessments were concordant with histopathologic findings in 87 of 89 margins assessed (one margin was uninterpretable and excluded), with diagnostic accuracy of 97.9% (kappa = 0.79). The sensitivity, specificity, PPV, and NPV were 100% (4/4), 97.6% (83/85), 66.7% (4/6), and 100% (83/83), respectively. **CONCLUSION**: US-OT was capable of providing distribution maps of lipid and Hb in lumpectomy specimens that predicted tumor margins with high sensitivity and specificity, making it a potential tool for intraoperative tumor margin assessment.

Translational Oncology (2020) 13, 254–261

Address all correspondence to: Malini Olivo, Singapore Bioimaging Consortium (SBIC), A*STAR Research Entities, 11 Biopolis Way, #02-02 Helios, Singapore 138667, Singapore. E-mail: Malini_Olivo@sbic.a-star.edu.sg
[1]Equal contributions.
Received 19 September 2019; Revised 6 November 2019; Accepted 11 November 2019

1936-5233/19
https://doi.org/10.1016/j.tranon.2019.11.005

Introduction

Breast-conserving surgery/therapy (BCS/BCT) that offers similar treatment benefits as total mastectomy, while retaining the breast shape and sensation [1,2] is now a standard treatment for early-stage breast cancer. However, the associated 20−40% chances of incomplete tumor excision (i.e., positive margins) [3−5] requiring patients to undergo a repeat operation is perceived as a drawback in the recovery of patient's mental well-being and a burden to hospital's resources. In current clinical practice, the reference standard for margin assessment is histopathologic examination of tissue which necessitates 24−48 h of sample fixation followed by days of sectioning and microscopic imaging. Routinely used clinical intraoperative strategies include tumor palpation, examining frozen tissue sections, imprint cytology, X-ray imaging, and ultrasonography, each of it possessing its own pros and cons [6]. While tumor palpation is associated with high interoperator variability and unsuitable for assessing nonmass forming cancers [7], frozen tissue sectioning [8] is expensive and time consuming and imprint cytology has low sensitivity and requires trained cytopathologist in the operation theater [9]. X-ray imaging, particularly specimen X-ray, while offering visualization of the complete specimen including clips and seeds in 2D, results in poor contrast between tumor and dense fibroglandular tissue [10]. Clinical deep-tissue ultrasonographic imaging, though proven to reduce reoperation rates and has been gaining popularity in intraoperative assessment of tumor margins [11,12] its inability to resolve tissue biochemical constituents makes it less attractive. Spot scanning techniques including the most recent FDA-approved radiofrequency spectroscopy-based "Margin Probe" offers potential, easy to use tool for margin detection but at the expense of sensitivity and specificity [6]. Several optical techniques that provide high-resolution molecular/biochemical imaging such as optical coherence tomography (OCT), Raman spectroscopy, fluorescence imaging, or recently developed spatial frequency domain imaging (SFDI) are continually developed to make BCS more successful [13−18]. However, optical techniques are more time-consuming to perform and are constrained by their limited depth of penetration (~3 mm) in tissues because of inherent light diffraction [6]. Hybrid modalities that take advantage of the superior tissue-level contrast attainable in optical imaging and the deep penetration of ultrasonography could therefore overcome the shortcomings of either imaging technology to obtain in-depth images of tissue structures that comes with contrasting details of tissue constituents such as hemoglobin and lipid.

Optoacoustic tomography (OT) is a hybrid optical-ultrasound technology based on the photoacoustic effect [19]. When short-pulsed laser of different wavelengths are beamed at tissues, light absorbing chromophores (e.g., lipid, water, hemoglobin) in the tissues expand and release thermoelastic acoustic waves which are detectable by an ultrasonic transducer. When these waves are captured, digitized, reconstructed, and spectrally unmixed, high-resolution (μm) distribution maps of the chromophores could be generated up to a depth of 3 cm [20]. The high spatial resolution and substantial depth of penetration make OT a potential tool for breast tumor margin assessment and is becoming an area of increasing interest [21,22]. As the breast is mostly composed of fat, the biochemical information from OT could potentially distinguish tumors (vasculature rich or fat-less) from normal breast tissue (fat-containing) [23]. Therefore, we hypothesize that ultrasound-guided optoacoustic tomography (US-OT) could be a potential tool for evaluation of tumor margins in lumpectomies. In this study, we sought to determine the diagnostic accuracy of US-OT in the assessment of tumor resection margins, using histopathology as reference standard.

Materials and Methods

Study Population and Participant Characteristics

This study was approved by our local institutional Domain Specific Review Board (DSRB). From February to June 2018, we prospectively screened 45 women (aged >18 years) referred to us for lumpectomy at the Department of Surgery, National University Hospital, Singapore. As US-OT is ultrasound-guided, women with lesions/tumors that were sonographically occult ($n = 14$) (e.g., ductal carcinoma in situ [DCIS] with mammographic microcalcifications only) were excluded from the study. Women with benign lesions (e.g., fibroadenoma) not requiring excision ($n = 6$) were also excluded. After obtaining written informed consent, the remaining 25 women were recruited into the study. Data obtained from the first 10 participants were used for training and optimization of image acquisition and processing, and that from the remaining 15 were used for analysis. The study timeline is shown in Figure 1.

Breast Cancer Specimen and Histopathology

After lumpectomy, the excised tissue was oriented by surgeons with silk stitches (Figure 2*A*) and then gently rinsed with saline to wash off surface blood. US-OT imaging was then performed on the specimen, following which it was placed in formalin and delivered to the laboratory to be sectioned and stained with hematoxylin and eosin (H&E) for histopathologic examination.

Equipment and Data Acquisition

For imaging of specimens, we used a custom-built two-dimensional (2D)−handheld optoacoustic probe adapted to a commercial multispectral optoacoustic tomography (MSOT) platform, the *MSOT inVision 512-echo* (iThera Medical GmbH, Munich, Germany). The probe consisted of an arc shaped (125 degree angular coverage) curvilinear array of 256 detector elements arranged on a spherical surface (radius 40 mm) and had a central frequency of 5 MHz (Figure 2*B*). The transducer has a bandwidth of 60% with the individual elements having a height of 13 mm and interelement pitch of 0.34 mm. To scan a specimen, the probe was mounted on a computer-controlled stage to touch the thickest portion of the specimen and from thereon moved across and up and down the specimen (placed on a silicone bed in an imaging chamber) through heavy water (D_2O) which provided good acoustic coupling (Figure 2*C*). Depending on the size, the probe was moved across the specimen as many times in steps of 1 mm to cover the entire specimen. Light transmitted via a fiber optic bundle integrated into the probe was delivered to the specimen in short pulses from a wavelength-tunable optical parametric oscillator (OPO) laser with selectable wavelengths (range, 660−1300 nm) at a repetition rate of 10 Hz and per-pulse energy of 37 mJ (at 750 nm). The resulting fluence on the sample surface was 3.17 mJ/cm^2. Illumination of the specimen excited light-absorbing chromophores within, which then emitted acoustic waves that was detected and captured by the US-OT probe. Acoustic signals were digitized and processed offline using model-based algorithm to reconstruct 2D cross-sectional images of

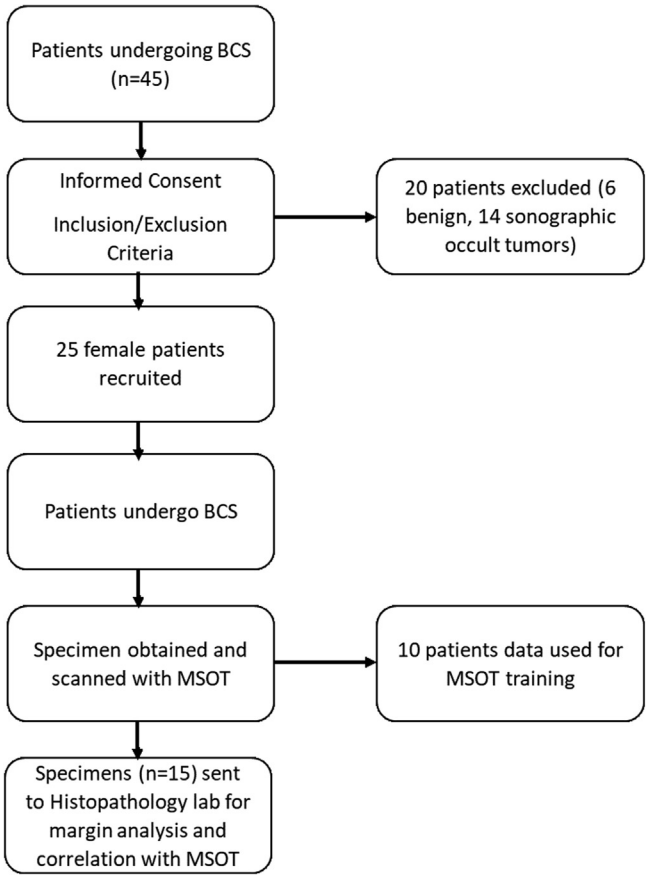

Figure 1. Schematic representation of the study protocol.

the tissue with an in-plane spatial resolution of 150 μm and effective field-of-view (FOV) of 25 × 25 mm. Images, averaging five frames per wavelength, were generated from data acquired at eight wavelengths: 710 nm, 730 nm, 760 nm, 800 nm, 850 nm, 930 nm, 1050 nm, and 1100 nm. During data acquisition, the real-time image generated by the back-projection algorithm was displayed on a preview window. To avoid damage to tissue, the light intensity in the probe was maintained to be within maximum permissible exposure limit set by the American National Standards Institute (ANSI).

Image Reconstruction and Analysis

Images acquired at each wavelength were reconstructed using a model-based algorithm [24]. Spectral unmixing was achieved by linear regression [25] to reveal the distribution of endogenous chromophores. Distribution maps for Hb and lipid were generated across the entire specimen. As each specimen contains six margins (anterior, posterior, superior, inferior, medial, and lateral), a total of 150 margins were assessed in excised specimens of 25 study participants. As part of training, US-OT images from the first 10 participants were assessed by consensus of three readers who were unblinded to histopathologic findings of the assessed margins: YG (breast radiologist with one year experience in OT), GB (three years' experience in clinical OT imaging) and MO (five years' experience in clinical OT imaging). Subsequently, US-OT images for the remaining 15 participants were assessed blinded to histopathologic findings, and independently by YG and GB, with any discordant readings resolved by MO.

Statistical Analysis

Results from margin assessments using US-OT were compared with histopathologic findings in a categorical format (i.e., positive/negative), with cross-tabulation performed for all assessed margins. Overall diagnostic accuracy, sensitivity, specificity, positive predictive value (PPV), and negative predictive value (NPV) of US-OT for diagnosis of margins were calculated by YH (20 years' experience in biostatistics) using the SPSS software (Version 22; PASW Statistics, Chicago, Ill). Kappa statistics were derived for overall agreement of US-OT with histopathology and for interobserver variation in assessment of US-OT images between YG and GB. As this was primarily a pilot proof of concept study, no sample size calculation was performed for the study.

Results

Patient Characteristics

Baseline characteristics, histopathology of breast tumors, volume, and scan times of lumpectomy specimens from 15 participants (mean

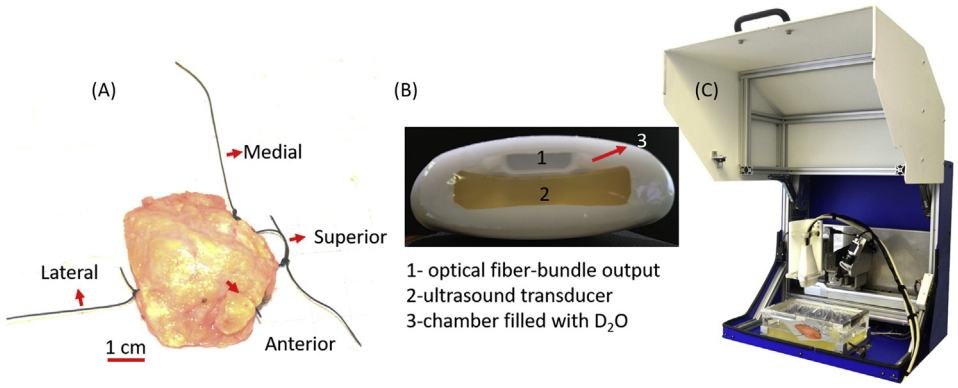

Figure 2. Instrumentation and sample preparation (A) Excised breast specimen margins labeled with silk stitches (Long stitch: Lateral margin, Medium length stitch: Medial margin, Short stitch: Superior margin, Loop stitch: Anterior margin). (B) Image of customized 2D handheld probe consisting of an arc shaped (125°) 2D array of 256 detector elements arranged on a spherical surface (radius 40 mm) with a centre frequency of 5 MHz. (C) Set-up of imaging chamber with probe mounted on a computer-controlled stage.

Table 1. Patient Characteristics and Results from Histopathology Analysis of Tumors for Tumor Markers and Size

Parameter	Value
Participant Characteristics	
Age, years	
Mean	52.7
Range	34−83
Histology	
DCIS (ductal carcinoma in situ)	1/15 (6.7%)
IDC (invasive ductal carcinoma)	6/15 (40%)
Combined IDC + DCIS	4/15 (26.7%)
ILC (invasive lobular carcinoma)	2/15 (13.3%)
Others (i.e., adenomyoepithelioma, papilloma with focus of DCIS)	2/15 (13.3%)
Pathologic Tumor Size, cm (Mean, Range)	
DCIS	0.3
IDC	1.5 (0.5−2.2)
Combined IDC + DCIS	2.1 (0.9−4.7)
ILC	1.1 (0.9−1.2)
Others	0.5
Tumor Markers	
ER+ DCIS	1
ER+ PR+ HER-2− IDC	6
ER+ PR+ HER-2− (combined IDC + ILC)	4
ER+ PR+ HER-2− (ILC)	2
ER+ DCIS (others)	1
Lumpectomy specimen volume, mls (mean ± SD)	168.0 ± 165.3
US-OT scan time, mm:ss (mean ± SD)	17:43 ± 05:50

age: 52.7 years ± 11.6 (SD)) included in the analysis are shown in Table 1 and Table S1.

US-OT Image Interpretation

US-OT imaging provided the tomographic ultrasound image and the optoacoustic distribution maps of Hb and lipid in the specimen. US-OT resolved lipid and blood signals up to a depth of 6 mm (data not shown). The 150 μm spatial resolution conferred by the 2D US-OT probe facilitated clear visualization of large blood vessels and continuity/discontinuity in lipid signals. In one representative case with negative margins seen on histology (Figure 3*B* and Figure S1), OT image of lipid distribution showed thick lipid layer on the margin surrounding the lesion (Figure 3*C*). In addition, OT image of Hb showed intense hemoglobin signals (yellow arrow in Figure 3*D*) around the edge of the lesion delineated by ultrasound. A merged image of lipid and hemoglobin distribution (Figure 3*E* and *F*) highlights the characteristics of a negative margin visualized by US-OT.

In a representative US-OT image of a positive margin (Figure 4 and Figure S2) confirmed by histopathology (Figure 4*B*), OT image of lipid distribution showed less intense lipid signals in between prominent and continuous lipid signals (Figure 4*D*) adjacent to the tumor lesion seen on ultrasound image. At the same time, the OT image of Hb distribution showed intense blood signals in the place of less intense lipid signals, suggesting the extension of feeding vessels outside of the tumor bulk (Figure 4*E*). A merged image of lipid and hemoglobin distribution (Figure 4*F*) highlights the characteristics of a positive margin visualized by US-OT. Therefore, on OT images, excised normal breast tissue appeared to be characterized by presence of intense and continuous lipid signal and absence of vascularity. Areas that contained less intense lipid signal with increased hemoglobin were noted as areas of tumoral angiogenesis or possible foci of DCIS. Based on histopathological examination, there was no evidence of laser-induced tissue damage to the excised breast specimen. The average scan time for each specimen in our study is approximately 20 min.

Data Analysis for Margin Assessment

In consensus with the acceptable margins set by Society of Surgical Oncology as having "no ink on tumor" for IDC (invasive ductal carcinoma) and a 2-mm negative margin for DCIS [26,27], we considered margins involved/positive when there was ≤2 mm of normal breast tissue seen between the tumor and the excised breast tissue margin of concern. Of the 90 margins from 15 participants that were assessed, one margin (inferior margin from participant 6) was excluded because of heavy staining by patent blue, rendering the OT image uninterpretable. Cross-tabulation results for the margins are shown in Table 2:

US-OT results were concordant with histopathologic findings for 87 of 89 margins assessed, with a high predictive accuracy of 97.9%. Two margins (1 anterior, 1 posterior) that were incorrectly assessed were false positives with histopathology showing extremely close negative margins at 0.5 mm and 1 mm, respectively. Overall, the study showed assessments by US-OT correlated well with histopathologic findings (kappa = 0.79). The sensitivity, specificity, PPV and NPV for detection of residual cancer were (4/4) 100%, (83/85) 97.6%, (4/6) 66.7%, and (83/83) 100%, respectively. There was no interpretive discrepancy between the two readers (YG and GB) for the 89 margins assessed (inter-observer variability = 1, kappa = 1).

Discussion

Many imaging modalities have been evaluated for use in intraoperative breast tumor margin assessments, including ultrasound, X-ray, and several optical methods, but each has its own limitation. Therefore, efforts are underway to develop an imaging system that could enable precise margin assessment within short intraoperative timescale to reduce current high reoperation rate in BCS. In the present study, we investigated the feasibility of using US-OT and determined its accuracy in assessing the margins of lumpectomy specimens. Our results show that US-OT provided clear visualization of large blood vessels and distribution of lipid and Hb in the lumpectomy specimens up to a depth of 6 mm. The sensitivity of US-OT to endogenous chromophores in the specimens enabled it to capture variations in lipid signal and increased vascularity in case of margin involvement. The clear optical contrast between different tissue biochemical constituents rendered it easy to discriminate positive and negative margins, resulting in highly accurate (97.9%) assessments of tumor margins. Unlike other optical techniques (e.g., fluorescence imaging), OT relies on differentiation of endogenous biochemical compounds by their optical absorption properties. Besides being label-free, US-OT is safe as we found no histopathologic evidence of laser-induced damage to the scanned specimens, indicating no risk of laser irradiation in the US-OT application. In addition, we were able to complete imaging of the entire specimen with an average scan time of 20 min per specimen. This is a fraction of the time required for histopathologic investigation of tissue specimen, and well below the recommended cold ischemia time of one hour [28]. All these suggest integrating US-OT in intraoperative clinical setting would facilitate timely decision on necessary tissue reexcision to ensure complete tumor-free margin in one single operation. This will potentially reduce or even eliminate the need for repeat surgical procedures which increase risks of patient's morbidity.

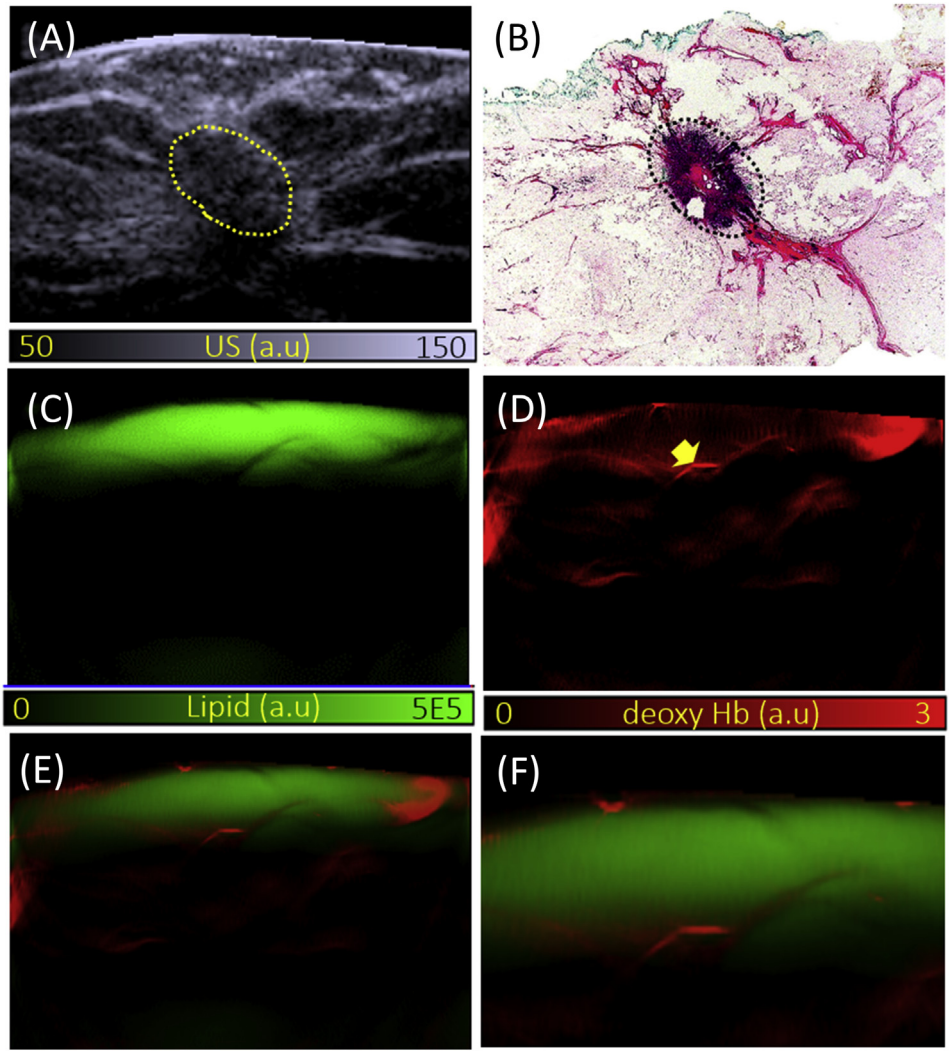

Figure 3. Ultrasound-guided optoacoustic tomography (US-OT) characteristics of negative tumor margins (A) Ultrasound image of specimen shows the hypoechoic tumor (IDC grade 2) (yellow circle) within the specimen (B) H&E stain of specimen shows the darkly stained tumor (black circle) with spiculated margins corresponding to the lesion seen on ultrasound. (C) Unmixed lipid signal demonstrating thick and intense lipid layer (>2 mm) between the tumor and the margin characteristic of negative margin. (D) Corresponding unmixed Hb signals in this region demonstrates vascularity in the tumor rim. (E—F) Merged and zoomed image of (C—D). Scale bar denotes 5 mm.

One of the challenges we faced during this study was the compression on the specimen exerted by the waterbed placed on its top that resulted in slight distortion and reduction in distance between the tumor and the anterioposterior margins, making evaluation difficult for cases with borderline cut-off values (i.e., 2 mm in our study). However, the false positives (1 anterior, 1 posterior) we encountered in US-OT assessment were not attributable to this distortion as histology demonstrated extremely close clear margins (0.5—1 mm). Despite these false positives resulting in a low PPV of 66.7%, overall agreement of US-OT assessment with histopathology remained good with a kappa value of 0.79.

Nevertheless, this feasibility study is not without limitations. Firstly, the limited effective FOV (25 × 25 × 20 mm) of the US-OT probe made it difficult to acquire data from a specimen in one sweep. In case of larger specimens, the sample or the stage had to be manually moved to scan the entire specimen, prolonging data acquisition times. Automating stage movement and developing algorithms to stitch the images could possibly speed up data acquisition times. Secondly, although the probe was able to resolve lipid and blood signals at a spatial resolution of 150 μm, the maximum depth it could reach was only 6 mm. This could be because of excised tissue being devoid of circulating blood, a dominant endogenous optical absorber that contributes to tissue contrast in optoacoustic imaging and lower laser power emitted at longer wavelengths (>900 nm). Nonetheless, the depth of optical penetration could be increased by modifying the light delivery (by means of transillumination), increasing the laser power or averaging of images, or by adjusting the dimensions of the transducer. Alternatively, a full ring ultrasound transducer array could be used to reveal a 360° view of the specimen in one sweep [29]. Thirdly, the sample size ($n = 15$) for this study was very small, secondary to the short study/funding period and the need to use substantial amount of specimens ($n = 10$) for model optimization and training purposes. Inclusion of more specimens, particularly those from denser breasts which are present in 40% of women [30] and posing severe challenges to specimen radiographic imaging technique will help to understand the performance of the US-OT technique and establish its robustness.

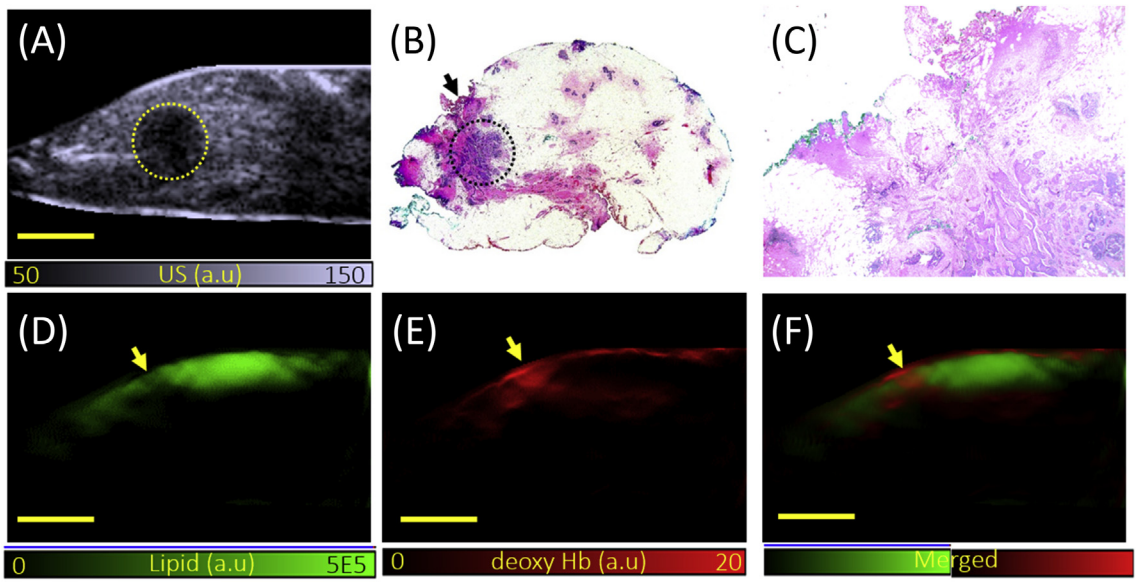

Figure 4. Ultrasound-guided optoacoustic tomography **(US-OT) characteristics of a positive margin.** (A) Ultrasound image of specimen shows the hypoechoic tumor (IDC grade 2) (yellow circle) near to the edge of the specimen at the lateral margins. (B) H&E stain of specimen at low power shows the darkly stained irregular tumor (black arrowhead) near to the lateral margins. (C) High power magnification view of the margin shows the index tumor (IT) with several tumor cells (red circle) extending to the cauterized lateral margin which is irregular and stained green (black arrowhead). (D) Unmixed lipid signal demonstrating disruption of the lipid layer at the lateral margin (yellow arrow). (E) Corresponding region shows increased evidence of vascularity on Hb distribution map suggestive of tumor extension. (F) Merged image of (D–E). Scale bar denotes 5 mm.

Nevertheless, according to the authors' knowledge, this study remains one of the first with the largest number of margins assessed ($n = 90$). Lastly, one margin was excluded from analysis owing to the heavy patent blue staining. Given that "no tumor at ink" is the current standard for pathologic assessment of negative surgical margins, this may pose a potentially very significant limitation of the clinical utility of US-OT in this setting. However, with the introduction of tunable OPO lasers that allows usage of multiple wavelengths to spectrally unmix endogenous contrast agents and a growing list of clinically used exogenous contrast agents [31,32], choosing the right

Table 2. Cross-Tabulation Table of Margins with Histology

Anterior Margin (15 Margins)		**Histology**	
		Positive	**Negative**
US-OT	Positive	0	1
	Negative	0	14
Posterior Margin (15 Margins)		**Histology**	
		Positive	**Negative**
US-OT	Positive	0	1
	Negative	0	14
Superior Margin (15 Margins)		**Histology**	
		Positive	**Negative**
US-OT	Positive	1	0
	Negative	0	14
Inferior Margin (14 Margins, 1 Excluded)		**Histology**	
		Positive	**Negative**
US-OT	Positive	1	0
	Negative	0	13
Medial Margin (15 Margins)		**Histology**	
		Positive	**Negative**
US-OT	Positive	0	0
	Negative	0	15
Lateral Margin (15 Margins)		**Histology**	
		Positive	**Negative**
US-OT	Positive	2	0
	Negative	0	13
Overall Margins (89 Margins)			
	Result	**95% CI (Lower)**	**95% CI (Upper)**
Sensitivity	100%	39.8%	100%
Specificity	97.7%	91.8%	99.7%
Positive predictive value	66.7%	33.7%	88.7%
Negative predictive value	100%	100%	100%
Accuracy	97.7%	92.1%	99.7%

wavelength during data acquisition and unmixing for ink will potentially circumvent the problem.

We conclude that the US-OT probe offered structural and functional information about margins of lumpectomy specimens with well-resolved tissue chromophores. The sensitivity of US-OT imaging to hemoglobin and lipid could be highly valuable for assessing tumor margins intraoperatively in a safe, rapid, and accurate manner. Good agreement of US-OT analysis with histopathologic interpretation makes it a potential tool for intraoperative margin assessment.

Funding

This work was supported in part by National Medical Research Council "Clinician Scientist Seed Fund" (Y.G.G) and A*STAR (Agency for Science, Technology and Research, Singapore) Biomedical Research Council intramural funds (M.O.).

Acknowledgements

The authors acknowledge Dr Jennie Wong from National University Singapore Medical & Scientific Communication department for proof-reading and editing the manuscript and SBIC-iThera Medical Imaging Centre for the imaging equipment.

Appendix A. Supplementary data

Supplementary data to this article can be found online at https://doi.org/10.1016/j.tranon.2019.11.005.

References

[1] Newman LA and Kuerer HM (2005). Advances in breast conservation therapy. *J Clin Oncol* **23**(8), 1685–1697. https://doi.org/10.1200/JCO.2005.09.046.

[2] Onitilo AA, Engel JM, Stankowski RV and Doi SA (2015). Survival comparisons for breast conserving surgery and mastectomy revisited: community experience and the role of radiation therapy. *Clin Med Res* **13**(2), 65–73. https://doi.org/10.3121/cmr.2014.1245.

[3] Atkins J, Al Mushawah F, Appleton CM, Cyr AE, Gillanders WE, Aft RL, Eberlein TJ, Gao F and Margenthaler JA (2012). Positive margin rates following breast-conserving surgery for stage I-III breast cancer: palpable versus nonpalpable tumors. *J Surg Res* **177**(1), 109–115. https://doi.org/10.1016/j.jss.2012.03.045.

[4] Fleming FJ, Hill AD, Mc Dermott EW, O'Doherty A, O'Higgins NJ and Quinn CM (2004). Intraoperative margin assessment and re-excision rate in breast conserving surgery. *Eur J Surg Oncol* **30**(3), 233–237. https://doi.org/10.1016/j.ejso.2003.11.008.

[5] Jacobs L (2008). Positive margins: the challenge continues for breast surgeons. *Ann Surg Oncol* **15**(5), 1271–1272. https://doi.org/10.1245/s10434-007-9766-0.

[6] Maloney BW, McClatchy DM, Pogue BW, Paulsen KD, Wells WA and Barth RJ (2018). Review of methods for intraoperative margin detection for breast conserving surgery. *J Biomed Opt* **23**(10), 1–19. https://doi.org/10.1117/1.jbo.23.10.100901.

[7] Balch GC, Mithani SK, Simpson JF and Kelley MC (2005). Accuracy of intraoperative gross examination of surgical margin status in women undergoing partial mastectomy for breast malignancy. *Am Surg* **71**(1), 22–27. discussion 27–28.

[8] Olson TP, Harter J, Munoz A, Mahvi DM and Breslin T (2007). Frozen section analysis for intraoperative margin assessment during breast-conserving surgery results in low rates of re-excision and local recurrence. *Ann Surg Oncol* **14**(10), 2953–2960. https://doi.org/10.1245/s10434-007-9437-1.

[9] Laucirica P (2005). Intraoperative assessment of the breast: guidelines and potential pitfalls. *Arch Pathol Lab Med* **129**(12), 1565–1574. https://doi.org/10.1043/1543-2165(2005)129[1565:iaotbg]2.0.co;2.

[10] Britton PD, Sonoda LI, Yamamoto AK, Koo B, Soh E and Goud A (2011). Breast surgical specimen radiographs: how reliable are they? *Eur J Radiol* **79**(2), 245–249. https://doi.org/10.1016/j.ejrad.2010.02.012.

[11] Doyle TE, Factor RE, Ellefson CL, Sorensen KM, Ambrose BJ, Goodrich JB, Hart VP, Jensen SC, Patel H and Neumayer LA (2011). High-frequency ultrasound for intraoperative margin assessments in breast conservation surgery: a feasibility study. *BMC Cancer* **11**, 444. https://doi.org/10.1186/1471-2407-11-444.

[12] Pan H, Wu N, Ding H, Ding Q, Dai J, Ling L, Chen L, Zha X, Liu X, Zhou W and Wang S (2013). Intraoperative ultrasound guidance is associated with clear lumpectomy margins for breast cancer: a systematic review and meta-analysis. *PLoS One* **8**(9):e74028. https://doi.org/10.1371/journal.pone.0074028.

[13] Busch DR, Choe R, Durduran T and Yodh AG (2013). Towards non-invasive characterization of breast cancer and cancer metabolism with diffuse optics. *PET Clin* **8**(3). https://doi.org/10.1016/j.cpet.2013.04.004.

[14] Flexman ML, Kim HK, Gunther JE, Lim EA, Alvarez MC, Desperito E, Kalinsky K, Hershman DL and Hielscher AH (2013). Optical biomarkers for breast cancer derived from dynamic diffuse optical tomography. *J Biomed Opt* **18**(9):096012. https://doi.org/10.1117/1.JBO.18.9.096012.

[15] Keller MD, Majumder SK, Kelley MC, Meszoely IM, Boulos FI, Olivares GM and Mahadevan-Jansen A (2010). Autofluorescence and diffuse reflectance spectroscopy and spectral imaging for breast surgical margin analysis. *Lasers Surg Med* **42**(1), 15–23. https://doi.org/10.1002/lsm.20865.

[16] Keller MD, Vargis E, de Matos Granja N, Wilson RH, Mycek MA, Kelley MC and Mahadevan-Jansen A (2011). Development of a spatially offset Raman spectroscopy probe for breast tumor surgical margin evaluation. *J Biomed Opt* **16**(7). https://doi.org/10.1117/1.3600708. 077006.

[17] Kennedy S, Geradts J, Bydlon T, Brown JQ, Gallagher J, Junker M, Barry W, Ramanujam N and Wilke L (2010). Optical breast cancer margin assessment: an observational study of the effects of tissue heterogeneity on optical contrast. *Breast Cancer Res* **12**(6), R91. https://doi.org/10.1186/bcr2770.

[18] Laughney AM, Krishnaswamy V, Rizzo EJ, Schwab MC, Barth Jr RJ, Cuccia DJ, Tromberg BJ, Paulsen KD, Pogue BW and Wells WA (2013). Spectral discrimination of breast pathologies in situ using spatial frequency domain imaging. *Breast Cancer Res* **15**(4), R61. https://doi.org/10.1186/bcr3455.

[19] Bell AG (1881). The production of sound by radiant energy. *Science* **2**(49), 242–253. https://doi.org/10.1126/science.os-2.49.242.

[20] Xia J, Yao J and Wang LV (2014). Photoacoustic tomography: principles and advances. *Electromagn Waves (Camb)* **147**, 1–22.

[21] Li R, Lan L, Xia Y, Wang P, Han LK, Dunnington GL, Obeng-Gyasi S, Sandusky GE, Medley JA, Crook ST and Cheng J-X (2018). High-speed intraoperative assessment of breast tumor margins by multimodal ultrasound and photoacoustic tomography. *Med Devices Sens* **1**(3):e10018. https://doi.org/10.1002/mds3.10018.

[22] Kosik I, Brackstone M, Kornecki A, Chamson-Reig A, Wong P, Araghi MH and Carson JJL (2019). Intraoperative photoacoustic screening of breast cancer: a new perspective on malignancy visualization and surgical guidance. *J Biomed Opt* **24**(5), 1–12.

[23] Goh Y, Balasundaram G, Moothanchery M, Attia A, Li X, Lim HQ, Burton N, Qiu Y, Putti TC and Chan CW, et al (2018). Multispectral optoacoustic tomography in assessment of breast tumor margins during breast-conserving surgery: a first-in-human case study. *Clin Breast Cancer 2018*. https://doi.org/10.1016/j.clbc.2018.07.026.

[24] Rosenthal A, Razansky D and Ntziachristos V (2010). Fast semi-analytical model-based acoustic inversion for quantitative optoacoustic tomography. *IEEE Trans Med Imaging* **29**(6), 1275–1285. https://doi.org/10.1109/TMI.2010.2044584.

[25] Razansky D, Distel M, Vinegoni C, Ma R, Perrimon N, Köster RW and Ntziachristos V (2009). Multispectral opto-acoustic tomography of deep-seated fluorescent proteins in vivo. *Nat Photonics* **3**, 412. https://doi.org/10.1038/nphoton.2009.98. https://www.nature.com/articles/nphoton.2009.98#supplementary-information.

[26] Moran MS, Schnitt SJ, Giuliano AE, Harris JR, Khan SA, Horton J, Klimberg S, Chavez-MacGregor M, Freedman G and Houssami N, et al (2014). Society of Surgical Oncology-American Society for Radiation Oncology consensus guideline on margins for breast-conserving surgery with whole-breast irradiation in stages I and II invasive breast cancer. *Ann Surg Oncol* **21**(3), 704–716. https://doi.org/10.1245/s10434-014-3481-4.

[27] Morrow M, Van Zee KJ, Solin LJ, Houssami N, Chavez-MacGregor M, Harris JR, Horton J, Hwang S, Johnson PL and Marinovich ML, et al

(2016). Society of Surgical Oncology-American Society for Radiation Oncology-American Society of Clinical Oncology consensus guideline on margins for breast-conserving surgery with whole-breast irradiation in ductal carcinoma in situ. *Pract Radiat Oncol* **6**(5), 287–295. https://doi.org/10.1016/j.prro.2016.06.011.

[28] Li X, Deavers MT, Guo M, Liu P, Gong Y, Albarracin CT, Middleton LP and Huo L (2013). The effect of prolonged cold ischemia time on estrogen receptor immunohistochemistry in breast cancer. *Mod Pathol* **26**(1), 71–78. https://doi.org/10.1038/modpathol.2012.135.

[29] Dean-Ben XL, Fehm TF, Ford SJ, Gottschalk S and Razansky D (2017). Spiral volumetric optoacoustic tomography visualizes multi-scale dynamics in mice. *Light Sci Appl* **6**(4):e16247. https://doi.org/10.1038/lsa.2016.247.

[30] Sprague BL, Gangnon RE, Burt V, Trentham-Dietz A, Hampton JM, Wellman RD, Kerlikowske K and Miglioretti DL (2014). Prevalence of mammographically dense breasts in the United States. *J Natl Cancer Inst* **106**(10), dju255. https://doi.org/10.1093/jnci/dju255.

[31] Ho CJH, Balasundaram G, Driessen W, McLaren R, Wong CL, Dinish US, Attia ABE, Ntziachristos V and Olivo M (2014). Multifunctional photosensitizer-based contrast agents for photoacoustic imaging. *Sci Rep* **4**, 5342. https://doi.org/10.1038/srep05342. https://www.nature.com/articles/srep05342#supplementary-information.

[32] Attia ABE, Balasundaram G, Driessen W, Ntziachristos V and Olivo M (2015). Phthalocyanine photosensitizers as contrast agents for in vivo photoacoustic tumor imaging. *Biomed Opt Express* **6**(2), 591–598. https://doi.org/10.1364/BOE.6.000591.